ENGINEERING JOURNAL

Seismic Shear Forces in Shear Walls of a Medium-Rise Building Designed By Response Spectrum Analysis

Ky Leng[1,a], Chatpan Chintanapakdee[1,b,*], and Toshiro Hayashikawa[2]

1 Department of Civil Engineering, Faculty of Engineering, Chulalongkorn University, Bangkok 10330, Thailand
2 Faculty of Engineering, Hokkaido University, Hokkaido, 060-8628, Japan
E-mail: [a]kyleng1986@yahoo.com, [b]chatpan.c@chula.ac.th (Corresponding author)

Abstract. According to ASCE7-05, response spectrum analysis (RSA) procedure can be used to determine the seismic demands of the structures for the seismic design of any type of structures. However, this design procedure has been found to be inappropriate for medium-rise and high-rise buildings. This paper is aimed at verifying the RSA procedure prescribed in the current Thai seismic design code which is based on ASCE7-05 and proposing appropriate modification to the design shear force from RSA procedure. A 16-story medium-rise reinforced-concrete core-wall case-study building was first designed based on RSA procedure and then the non-linear response history analysis (NLRHA) was performed to determine the more accurate seismic demands of the structure. The results show that seismic shear demand of the shear wall from non-linear analysis is about 2 times the shear capacity of the wall designed by RSA procedure. This could lead to shear failure in the shear walls designed by RSA procedure. To avoid shear failure in the shear wall elements, the shear demands in the wall elements designed by RSA procedure needs to be amplified by a factor of 2, which is equivalent to reducing the response modification factor R = 5.5 in ASCE7-05 to R = 2.75 (for shear force in the shear wall only).

Keywords: Seismic shear demand, medium-rise building, response spectrum analysis, nonlinear response history analysis.

ENGINEERING JOURNAL Volume 18 Issue 4
Received 2 September 2013
Accepted 16 June 2014
Published 16 October 2014
Online at http://www.engj.org/
DOI:10.4186/ej.2014.18.4.73

DOI:10.4186/ej.2014.18.4.73

1. Introduction

Medium-rise and high-rise concrete core-wall buildings have been used intensively due to its lower costs and faster construction compared with other medium-rise and high-rise buildings using other lateral-force-resisting system [1]. For this kind of building system, the lateral-force-resisting system is normally provided by the core wall, since it is much stiffer than the column frame. For economical reason, the building is expected to behave non-linearly and capacity design concept may be applied, then the desired mechanism is that the flexural plastic hinge is formed near the base of the core wall and flexural yielding is anticipated in the coupling beam.

However, the current code provision does not distinguish the requirements for the design of low-rise, medium-rise and high-rise buildings, and this may lead to less-than-desirable result.

In design practice, the equivalent static design procedure, in which the first mode of the structure is assumed to dominate, is generally used for low-rise regular structures due to its simplicity. However, for long-period structure like tall building, the seismic response of higher modes contributes significantly. The equivalent static procedure is thus found to be inappropriate. Hence, another approach known as response spectrum analysis (RSA), which accounts for multi-mode effects, is employed in the current Thai seismic design code [2] (based on ASCE7-05 [3]). In the RSA procedure, to determine the seismic demands of the structure due to earthquake loading, we first compute the elastic responses of each vibration mode from dynamic analysis and the design response spectrum in the code based on 5% damping ratio and then the responses of each mode are combined by either the square-root-of-sum-of-squares (SRSS) or the complete quadratic combination (CQC) rule [4], finally the total elastic responses are reduced to the seismic demands for structural design by a response modification factor "R" that accounts for the over-strength and inelastic effects of the structure.

Despite the fact that RSA procedure is currently allowed by the code provision, many researchers have found that RSA procedure prescribed in the current design code can sometimes lead to unsafe design since it cannot capture the actual behavior of tall building under seismic loading. By using a 40-story reinforced concrete core wall building, Zekioglu et al. [5] has shown that the seismic shear strength of the core wall segments and coupling beams should be determined by NLRHA. Moreover, they found that the seismic shear demand over the entire height of the wall from NLRHA based on maximum considered earthquake (MCE) is as high as 5 times the corresponding demands from RSA procedure based on design basis earthquake (DBE) level of excitation. Another similar investigation conducted by Tuan [6] using a 45-story reinforced concrete frame wall building has also revealed that the DBE seismic demands (shear and moment) over the entire height of the wall from NLRHA are about 1.5 times the corresponding demands obtained from RSA procedure. Other similar findings done by Klemencic et al. [7] and Sangarayakul and Warnitchai [8] have also confirmed the insufficiency of RSA procedure on tall buildings. More recently, Munir and Warnitchai [9] studied and explained the causes of unsafe design by RSA procedure based on a 40-story case study building, three main differences in both analyses (RSA and NLRHA) such as: damping ratio, level of ground motion (DBE and MCE), and material over-strength used only in NLRHA were considered. And despite these differences were adjusted and made the same, the seismic shear demand from NLRHA is still about 1.5 times the corresponding demand from RSA procedure.

In this paper, based on a case study of a medium-rise core-wall concrete building located in Bangkok, Thailand, we aim to verify the response spectrum analysis procedure prescribed in the current Thai seismic design code [2], to identify the weak points of structural members (shear wall and column), and finally to make appropriate suggestions for improvement of the current Thai seismic design code [2] to address the design of medium-rise buildings.

The case-study building was first analyzed by RSA procedure using ETABS [10]. The resulted seismic demands were used to design the shear walls and columns such that the nominal strengths of the members were greater than or equal to the demands divided by appropriate strength reduction factors per ACI318-08 [11]. The building already designed by RSA procedure was then analyzed again using NLRHA procedure through PERFORM-3D [12], in which a set of seven earthquake ground motions was input as seismic loading. Finally, the demands from both RSA and NLRHA were compared to check the validity of RSA procedure and the deformations of the structural members due to NLRHA were checked against the allowable limit in ASCE41-06 [13].

2. Structural system

The case-study building is a 16-story reinforced-concrete building which is 49.2 m tall with 43.2 x 18.6 m floor plan (Fig. 1). The lateral-load-resisting system of the building consists of reinforced-concrete core walls and slab-column frames, whereas the gravity-load-carrying system comprises 18-cm thick post-tensioned concrete flat slab resting on reinforced concrete columns and shear walls. The column cross section is 90 cm x 30 cm and the walls are 25 cm thick. The compressive strength of concrete is 32 MPa, and yielding strength of steel rebar is 400 MPa. Young modulus of concrete and steel are 28,600 MPa and 200,000 MPa, respectively.

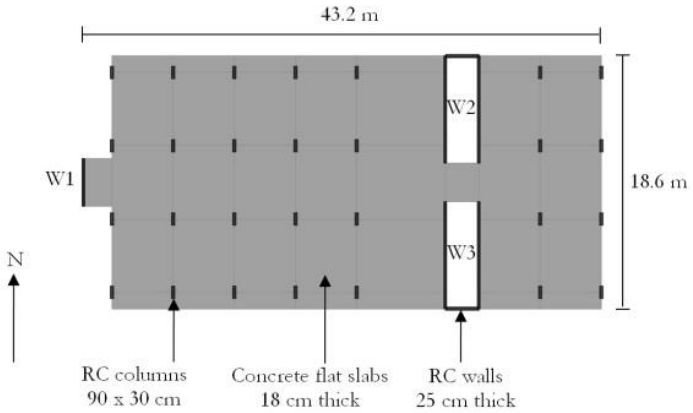

Fig. 1. Typical floor plan.

3. Linear model for response spectrum analysis (RSA)

For linear analysis, floor slabs were assumed to be rigid diaphragms where the floors are rigid in plane and flexible out of plane. The effective stiffness of structural members was based on the value provided in the Thai seismic design code [2] as shown in Table 1. The columns were modeled as linear frame elements, while slabs and walls were modeled as shell elements as illustrated in Table 2. The finite element model of the studied structure in ETABS [10] is shown in Fig. 2.

Table 1. Effective stiffness of the structural members.

Structural elements	Effective stiffness
Columns	$I_{eff} = 0.70\ I_g$
Walls	$I_{eff} = 0.70\ I_g$
Slabs	$I_{eff} = 0.25\ I_g$

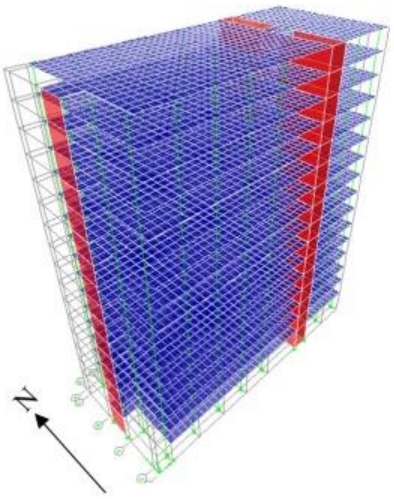

Fig. 2. Building model in ETABS [10].

DOI:10.4186/ej.2014.18.4.73

Table 2. Types of elements used for linear and nonlinear models.

Structural Elements	Linear Model (ETABS)	Nonlinear Model (PERFORM-3D)
Column	Frame element	Frame element + plastic hinges at both ends
Wall	Shell element	Inelastic fiber section
Slab	Shell element	Shell element

4. Nonlinear model for nonlinear response history analysis (NLRHA)

For NLRHA in PERFORM-3D [12], the columns were modeled as reinforced-concrete column elements, which consist of linear components with nonlinear plastic hinges at both ends of each member. The hinge yield strength is defined by three-dimensional P-M-M yield surface. Fig. 3 shows the tri-linear moment-rotation relationship of the plastic hinge as available in PERFORM-3D. Point Y represents the first yield; point U is the ultimate strength; point R is residual strength; and point X represents maximum deformation. The parameters for the tri-linear relationship including hinge rotation capacity and yield moment can be found in Haselton et al. [14], and Panagiotakos and Fardis [15], respectively. Linear elastic shell elements were used for the post-tensioned flat slab.

Inelastic fiber-section models were used for reinforced-concrete shear walls throughout the entire height. A fiber-section segment consists of eight concrete fibers along with eight equally spaced steel fibers (Figs. 4 and 5). Each story of the W1 wall was modeled with one segment of fiber section (Fig. 4), whereas the cross section of W2 and W3 walls consists of three segments (Fig. 5). All concrete fibers in one segment of W1 were modeled as unconfined concrete (Fig. 4), whereas concrete fibers in the boundary regions of W2 and W3 were modeled as confined concrete and the middle region as unconfined concrete (Fig. 5)

Steel fibers in W1 have uniform cross-sectional area (Fig. 4), whereas steel fibers in the boundary regions of W2 and W3 are larger than in the middle region (Fig. 5). The cross-sectional areas of steel fibers in all walls are shown in Table 3. The whole structure model in PERFORM-3D [12] is illustrated in Fig. 6.

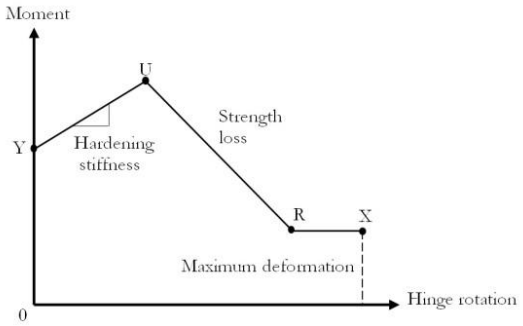

Fig. 3. PERFORM-3D moment-rotation relationship of plastic hinges in column element [12].

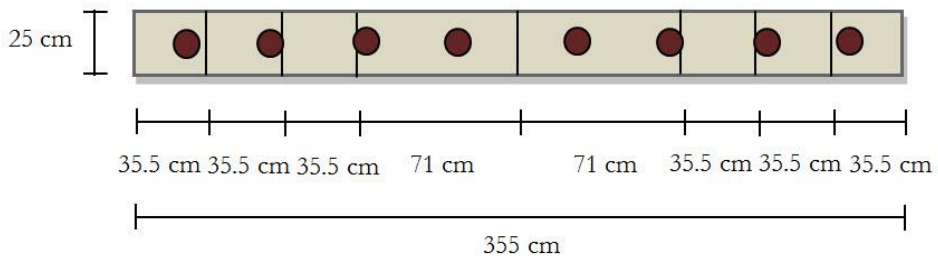

Fig. 4. Fiber section model of W1 wall.

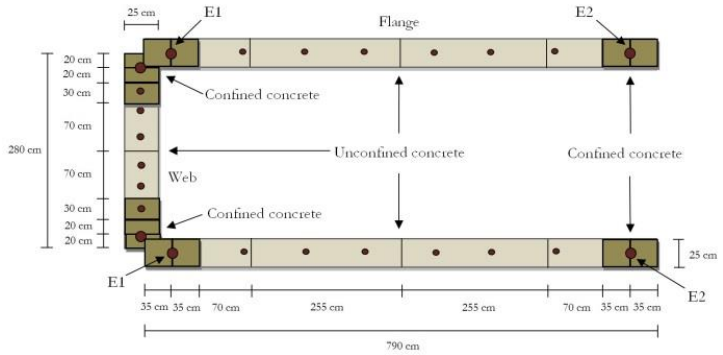

Fig. 5. Fiber section of W2 and W3.

Table 3. Area of each steel fiber.

Story	Area of each steel fiber (cm²)					
	W1	W2 and W3				
		Web		Flange		
		Boundary	Middle	Boundary (E1)	Boundary (E2)	Middle
1	11.65	95.43	1.131	127.23	95.43	4
2	6.66	57.73	1.131	76.97	57.73	4
3	3.33	42.41	1.131	76.97	42.41	4
4	3.33	42.41	1.131	56.55	42.41	4
5	3.33	36.95	1.131	49.26	36.95	4
6	3.33	29.45	1.131	39.27	29.45	4
7	3.33	29.45	1.131	39.27	29.45	4
8	3.33	29.45	1.131	39.27	29.45	4
9	3.33	18.85	1.131	25.13	18.85	4
10	3.33	18.85	1.131	25.13	18.85	4
11	3.33	12.06	1.131	16.08	12.06	4
12	3.33	9.24	1.131	12.32	9.24	4
13	1.665	9.24	1.131	12.32	9.24	4
14	1.665	1.54	1.131	3.08	1.54	4
15	1.665	1.54	1.131	3.08	1.54	4
16	1.665	1.54	1.131	3.08	1.54	4

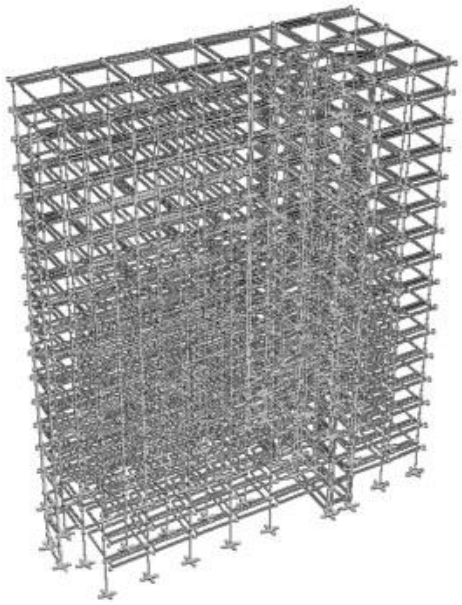

Fig. 6. Building model in PERFORM-3D [12].

4.1. Material Models

The stress-strain relationships of confined and unconfined concrete used in this study referred to the models proposed by Reddiar [16], which is similar to the well-known Mander et al. [17] except for the descending branch of stress-strain curve. Both models assume that concrete resist no tensile stress. Reddiar models had to be approximated as a tri-linear relationship due to limitation in PERFORM-3D [12]. The approximation was implemented such that the area under the curves remains unchanged. Fig. 7(a) and (b) show the stress-strain relationship of unconfined and confined concrete, respectively.

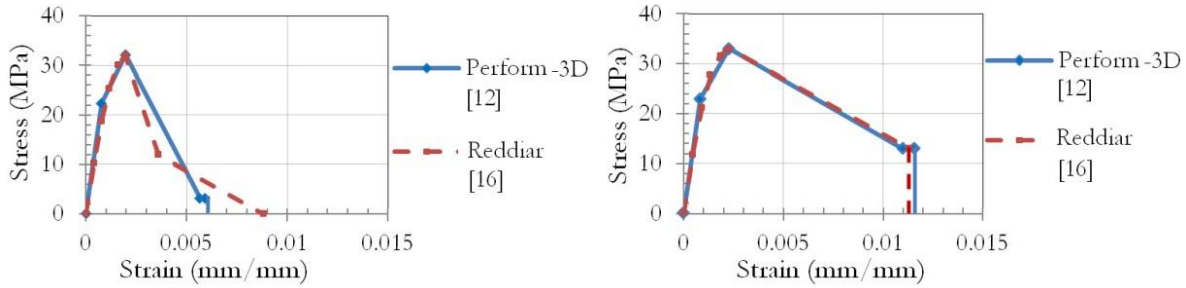

Fig. 7. Concrete stress-strain relationships.

The reinforcing steel stress-strain relationship is based on material specification for steel rebar and modeled with nominal yield strength of 400 MPa and ultimate strength of 570 MPa, as shown in Fig. 8.

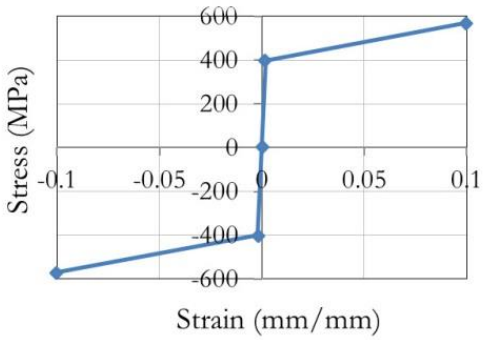

Fig. 8. Steel stress-strain relationship.

The types of elements used for linear and nonlinear models are summarized in the Table 2 above. Different models were used for columns and shear walls; the columns were modeled as elastic frame elements in ETABS while elastic frame elements with plastic hinges at both ends were utilized to model the columns in PERFORM-3D. The walls were modeled as shell elements in ETABS and as inelastic fiber section components in PERFORM-3D. The slabs were modeled as shell elements in both ETABS and PERFORM-3D.

4.2. Hysteretic Model

The monotonic curve is first input into PERFORM-3D [12], and then the cyclic behavior of the components is determined by specifying the energy dissipation factor, which is defined as the area of degraded hysteretic loop divided by the area of non-degraded loop. PERFORM-3D [12] adjusts the unloading and reloading stiffness to reduce the area under the loop according to the input energy dissipation factor. The values of the energy degradation factors are shown in Table 4. These values are obtained from doing trial and error by Kaewnurachadasorn [18] to get the best match with the experimental results for hysteretic loop of columns in Sezen [19].

Table 4. Cyclic degradation in PERFORM-3D [12].

Point	Energy factor
Y	0.5
U	0.3
L	0.2
R	0.05
X	0.05

Degraded loop for trilinear behavior is used for the hysteretic model of the column components as shown in Fig. 9 and Fig. 10. In Fig. 9, the dash lines represent the first cyclic behavior of the components before the deformations of the components in both positive and negative branches reach U (ultimate) point, whereas the solid lines are the second cyclic behavior of the components in two extreme shapes for the degraded loop; (a) minimum elastic range, this extreme case gives minimum elastic range and maximum strain hardening range. The elastic stiffness remains the same as the first cycle, but the yielding strength of the component reduced and the strain hardening stiffness also degraded. The hardening stiffness is calculated to make the area of the degraded loop equal to the energy degradation factor times the area of the non-degraded loop (first cycle). (b) Maximum elastic range, this extreme case gives maximum elastic range and minimum strain hardening range. The hardening stiffness does not change while the elastic stiffness degraded such that the area of the degraded loop is equal to the energy degradation factor times the area of the non-degraded loop (first cycle). In Fig. 10, the dash lines represent the first cyclic behavior of the components after the positive and negative deformations of the components attain U point, whereas the solid lines are the second cyclic behavior of the components for the degraded loop. The yield strength of the components degraded, the elastic and strain hardening stiffness degraded and are computed to make the area of the degraded loop equal to the energy degradation factor times the area of the non-degraded loop (first cycle).

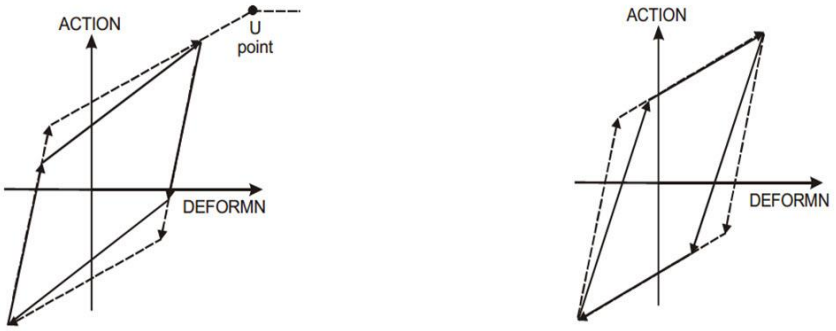

(a) Minimum elastic range. (b) Maximum elastic range.

Fig. 9. Degraded loop for trilinear behavior before U point in PERFORM-3D [12].

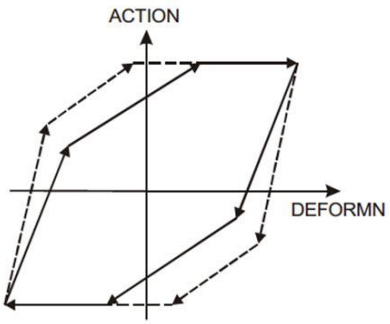

Fig. 10. Degraded loop for trilinear behavior after U point in PERFORM-3D [12].

Similarly, the degraded loop for concrete fiber of the shear wall fiber section is shown in Fig. 11.

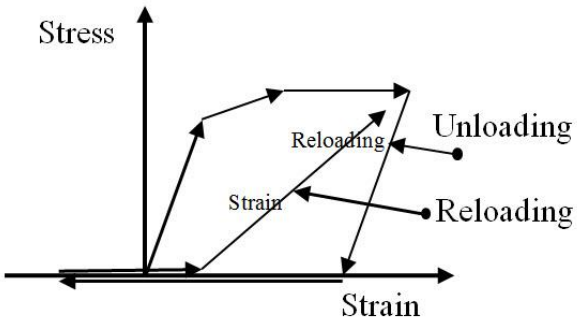

Fig. 11. Hysteretic model for concrete fiber in compression in PERFORM-3D [12].

4.3. Response Spectrum and Ground Motions

A set of ground motion records representing maximum considered earthquake (MCE) having 2% probability of exceedence in 50 years (2475 years return period) is selected for NLRHA. This set of ground motions consists of 7 records, as illustrated in Table 5, and was input into ProShake software [20] to simulate the wave propagation through soft soil layers underlying Bangkok. The resulted ground motions are used for NLRHA and shown in Fig. 12. The pseudo-acceleration spectra for this set of ground motions output from ProShake [20] for 5% damping ratio are shown in Fig. 13 together with the average spectrum (black bold solid line).

Table 5. Selected ground motion records.

No.	Earthquake event	Station	Magnitude	Distance (km)	PGA (g)	Duration (s)
1	1999 Kocaeli	Maslak	7.4	64	0.165	143
2	1999 Chi-Chi	TTN 042	7.6	65	0.128	111
3	1994 Northridge	Wrightwood-Jackson Flat	6.7	68	0.154	74
4	1989 Loma Prieta	Piedmont Jr High	6.9	73	0.122	65
5	1971 San Fernando	Cedar Springs-Allen Ranch	6.6	90	0.142	41
6	1999 Chi-Chi	TAP 077	7.6	117	0.074	103
7	1992 Landers	San Gabriel-E Grand Ave	7.3	142	0.120	72

Note: PGA = Peak Ground Acceleration

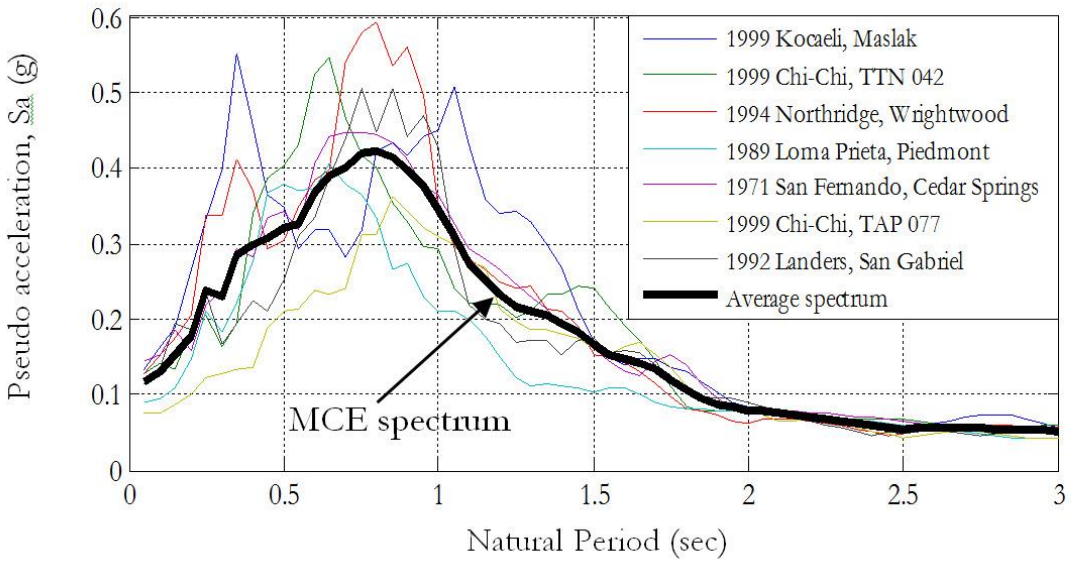

Fig. 12. List of the seven ground motions used in NLRHA (Faculty of Engineering, [21]).

The design response spectrum used in RSA procedure should be the spectrum that represents design basis earthquake (DBE), which is defined as 2/3 of the MCE spectrum and is obtained from the average spectrum of the seven records multiplied by 2/3 presented earlier. It is plotted in Fig. 14 (R_{eff} = 1).

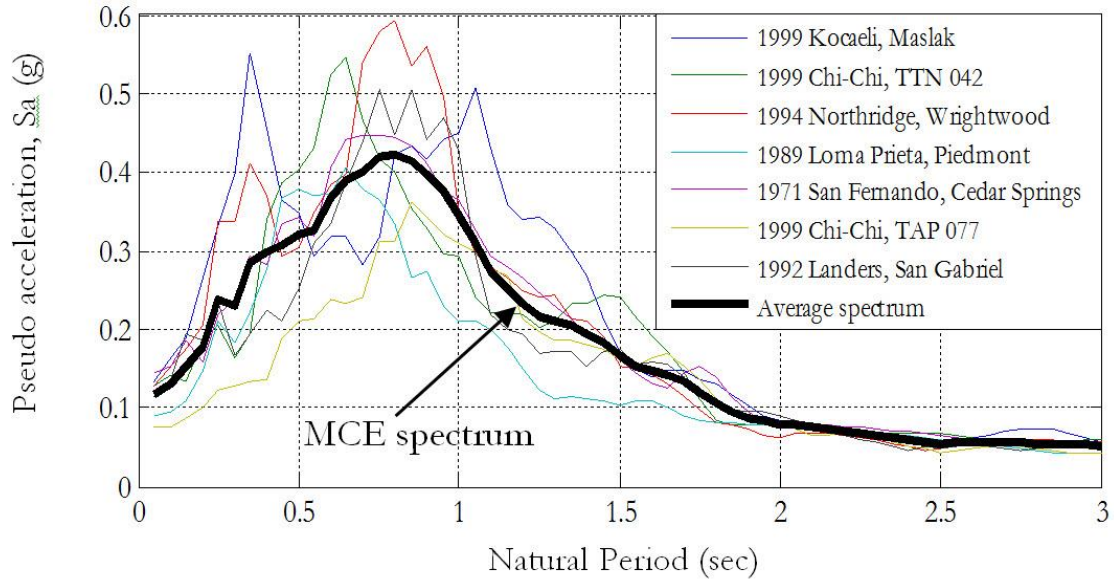

Fig. 13. Pseudo-acceleration spectra for the set of seven ground motions (MCE).

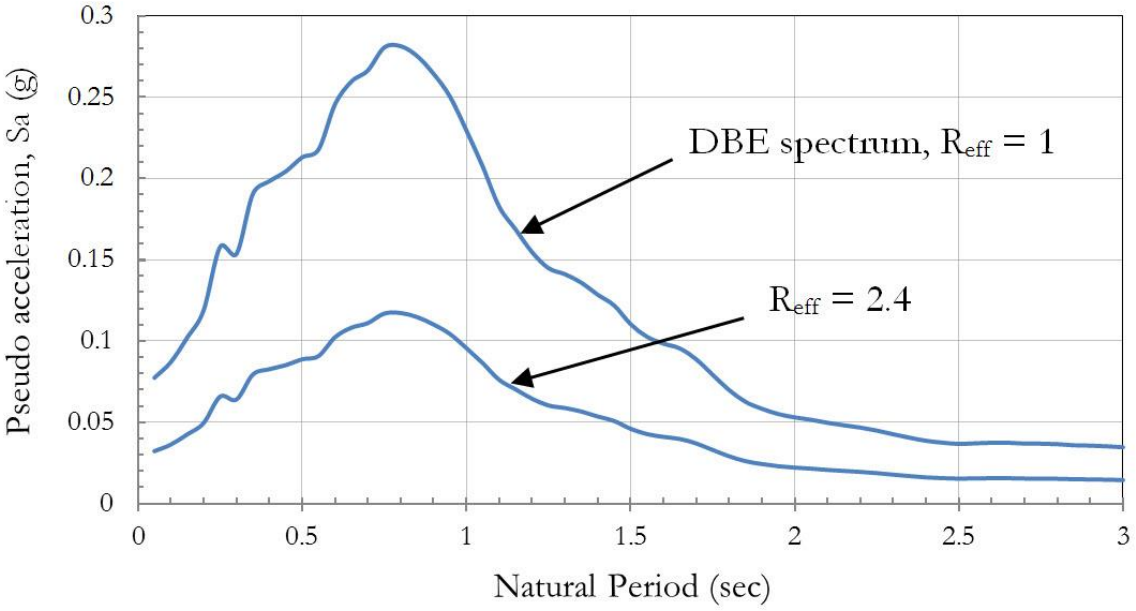

Fig. 14. Design response spectrum (DBE) with Reff = 1 and Reff = 2.4.

5. Results

5.1. Response Spectrum Analysis

In this analysis, the elastic responses of all significant vibration modes (20 modes) are first determined using the design response spectrum in Fig. 14 (R_{eff} = 1), and then combined into total responses by CQC rule, finally reduced by a seismic modification factor (R/I). The "R" factor of 5.5 is selected since the building is categorized as ordinary reinforced concrete shear wall structure and important factor I=1.25 for occupancy

category III [3]. The analysis has been conducted via ETABS [10] considering both P-delta and accidental torsional (5% eccentricity) effects. The modal properties of the building structure are shown in Table 6.

Table 6. Modal properties of the building.

Mode	Modal natural period (sec)	Modal mass contribution in E-W (%)	Modal mass contribution in N-S (%)
1	2.92	69.81	0
2	2.86	0	25.36
3	1.30	0	42.21

The drift ratio obtained from the analysis is multiplied by a factor of 3.6 (C_d/I) required by the code [3]. The deflection amplification factor C_d of 4.5 is selected corresponding to R=5.5. As illustrated in Fig. 15, the maximum story drift ratio throughout the entire height of the building is about 0.5%, which is only 1/3 of the allowable drift ratio prescribed in the code [3].

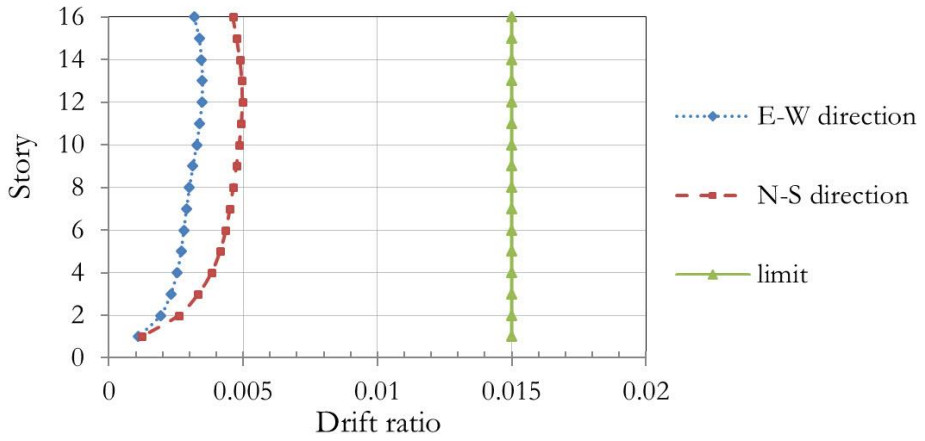

Fig. 15. Story drift ratios in RSA procedure – RSA procedure versus Allowable limit.

5.1.1. Equivalent lateral force procedure

Thai seismic design code [2] (based on ASCE7-05 [3]) required that seismic design base shear obtained from linear RSA procedure be not less than 85% of the base shear evaluated from linear static analysis, which is the equivalent lateral force (ELF) procedure. Table 7 summarizes the ELF procedure.

Table 7. Summary of equivalent lateral force procedure.

Parameters	Value
Important factor : I	1.25
Seismic modification coefficient : R	5.5
Code period in E-W direction : T	1.476 s
Code period in N-S direction : T	1.300 s
Seismic response coefficient in E-W direction : Cs	0.0257 g
Seismic response coefficient in N-S direction : Cs	0.0318 g
Effective weight of the building : W	10855 ton
Seismic base shear in E-W direction : V_{static}	2790 kN
Seismic base shear in N-S direction : V_{static}	3450 kN

5.1.2. Seismic demand from RSA procedure

Since the seismic base shear ($V_{dynamic}$) first calculated from RSA procedure is less than 85% of seismic base shear (V_{static}) from ELF procedure as shown in Table 8, the force demands need to be scaled up such that the $V_{dynamic}$ from RSA procedure is equal to $0.85V_{static}$. To satisfy this requirement, the RSA has been

performed again via ETABS [10] with effective seismic modification "R_{eff}" replacing the "R/I" factor, in which R_{eff} is defined as the smaller of R/I multiplied by $V_{dynamic}/0.85V_{static}$ and R/I as illustrated in Table 8. The response spectrum divided by R_{eff} is plotted in Fig. 14 (R_{eff} = 2.4). It should be noted that the shear wall: W2 and W3 are symmetric so the same demands throughout the entire height of the walls are expected, thus the following results will be shown only for W2.

Table 8. Seismic base shear of ELF and RSA procedure.

Parameters	**Value**
ELF procedure	
85% of Seismic base shear in E-W direction : $0.85V_{static}$	2371 kN
85% of Seismic base shear in N-S direction : $0.85V_{static}$	2932 kN
RSA procedure	
Seismic base shear in E-W direction : $V_{dynamic}$	1310 kN
Seismic base shear in N-S direction : $V_{dynamic}$	1570 kN
R_{eff} = min { R/I * $V_{dynamic}/0.85\ V_{static}$, R/I }	
For E-W direction	2.43
For N-S direction	2.36

Therefore the seismic demands of structural members of the building are calculated based on this new seismic modification factor R_{eff} and shown in Fig. 18 through Fig. 23. The structural walls and columns are designed such that their nominal strength multiplied by a strength reduction factor in ACI318-08 [11] code is approximately equal to the seismic demands from RSA procedure mentioned earlier.

5.2. Nonlinear Response History Analysis

Nonlinear time history analysis has been performed through PERFORM-3D [12] considering P-delta effect with two levels of ground motions: (1) DBE ground motion and (2) MCE ground motion both consisting of seven records. It should be noted that the seven MCE ground motion records are obtained from site response analysis of Bangkok soft soil using the records shown in Table 5 as input ground motions and DBE records are obtained from multiplying the MCE records by 2/3. These two levels of ground motions were applied separately in both horizontal directions to the building, namely North-South and East-West directions.

5.2.1. Verification of RSA procedure

In this study, DBE ground motions are used in NLRHA. The average value of maximum story drift ratio obtained from NLRHA using the seven DBE ground motions and the maximum story drift ratio calculated from RSA procedure are compared and shown in Fig. 16 and Fig. 17. We can see from these figures that RSA procedure underestimates drift ratios in E-W direction, which is predominated by the frame action, and overestimates drift ratio in N-S direction, which is predominated by the wall action.

The same comparison is made between the mean values of demands from NLRHA and from RSA procedure for the forces in walls. As shown in Fig. 18 and Fig. 19, RSA procedure underestimates the seismic shear demands throughout the entire height of W1 and the moment at middle stories of W1 (from story 4 to 10).

DOI:10.4186/ej.2014.18.4.73

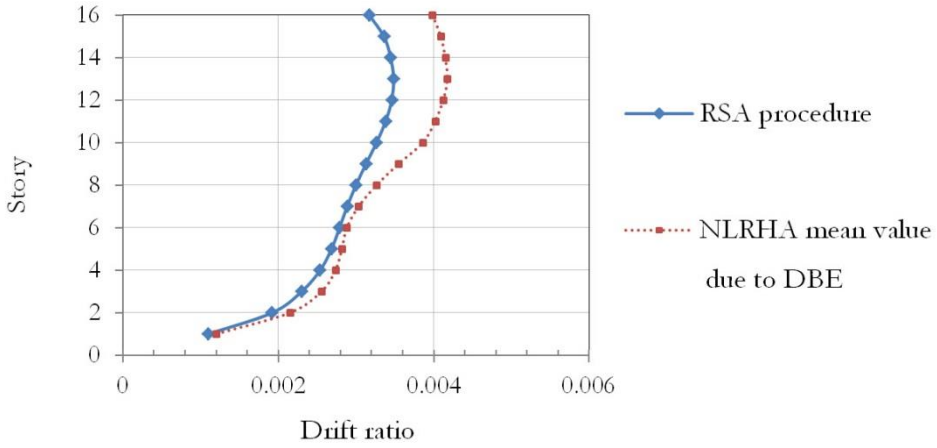

Fig. 16. Maximum story drift ratios in E-W direction – RSA versus NLRHA procedure due to DBE.

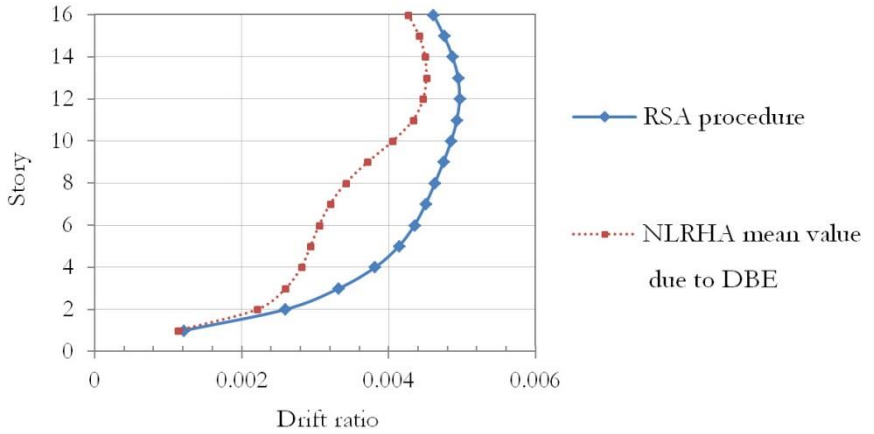

Fig. 17. Maximum story drift ratios in N-S direction - RSA versus NLRHA procedure due to DBE.

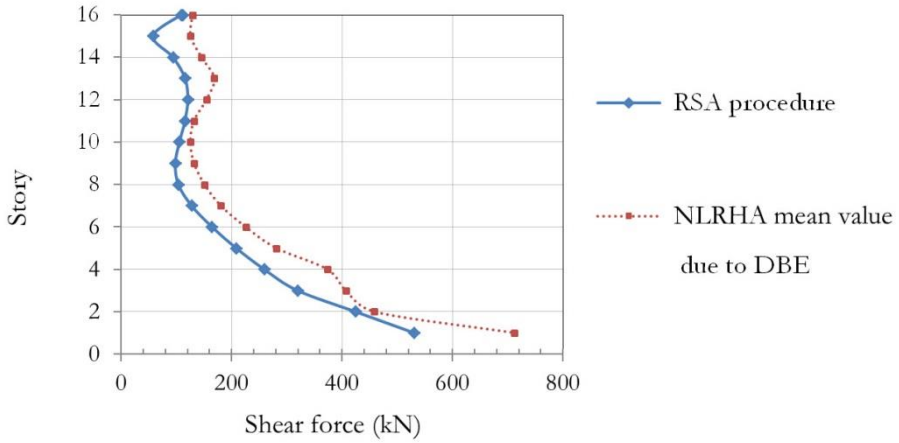

Fig. 18. Shear force in W1 - RSA versus NLRHA procedure due to DBE.

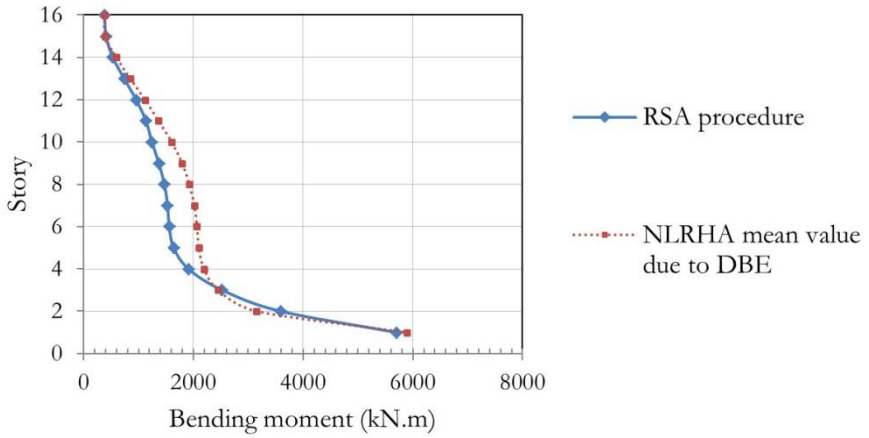

Fig. 19. Bending moment in W1 - RSA versus NLRHA procedure due to DBE.

It can be seen from Fig. 20 and Fig. 21 that the seismic shear demands of W2 from NLRHA procedure are about 2 times as high as the corresponding shear demands from RSA procedure and that their distribution patterns throughout entire height are almost the same. These results agree quite well with the results of Klemencic et al. [7], and Munir and Warnitchai [9]. Similarly, the bending moment from NLRHA is also about 2 times the corresponding demands from RSA procedure throughout the entire height of the building as depicted in Fig. 22 and Fig. 23. There are three main reasons contributing to the differences of bending moment in both RSA and NLRHA. Firstly, the strength reduction factor of 0.9 used in the design process makes the structure for NLRHA 10% stiffer. Secondly, the P-M2-M3 interaction effect increases the yield moment by about 2 times. Lastly, the material strain hardening used in steel model for NLRHA can also increase the bending moment in NLRHA after yielding occur. Thus even though the seismic moment in NLRHA is as high as 2 time the corresponding demand in RSA procedure, the walls still perform well in flexure without excessive wall rotation as presented later in this report (Table 9).

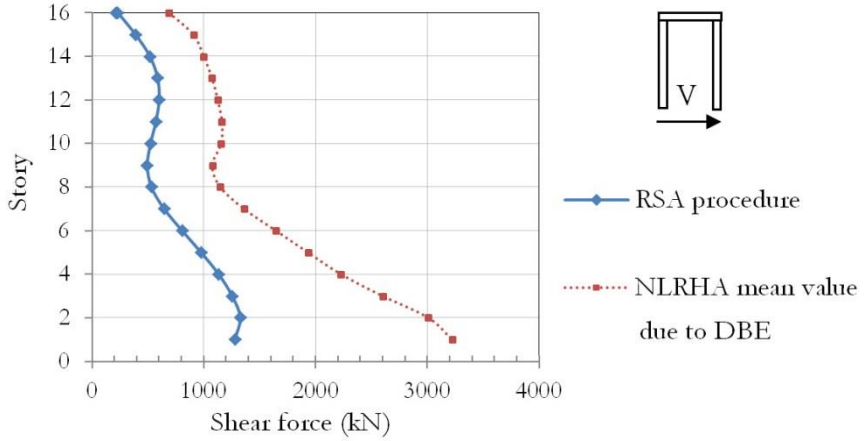

Fig. 20. Shear force in W2 – E-W direction - RSA procedure versus NLRHA due to DBE.

DOI:10.4186/ej.2014.18.4.73

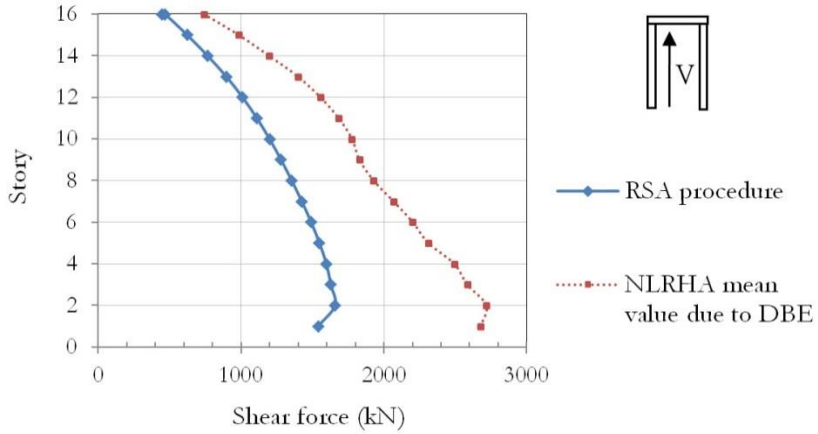

Fig. 21. Shear force in W2 – N-S direction – RSA procedure versus NLRHA due to DBE.

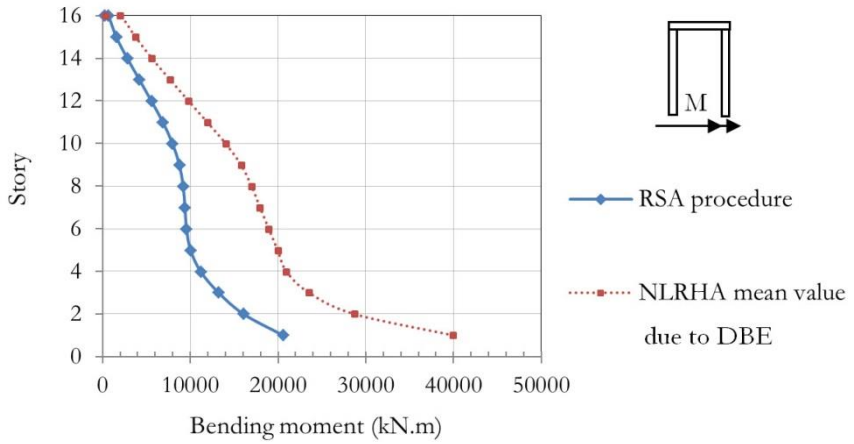

Fig. 22. Bending moment in W2 – about N-S direction – RSA procedure versus NLRHA due to DBE.

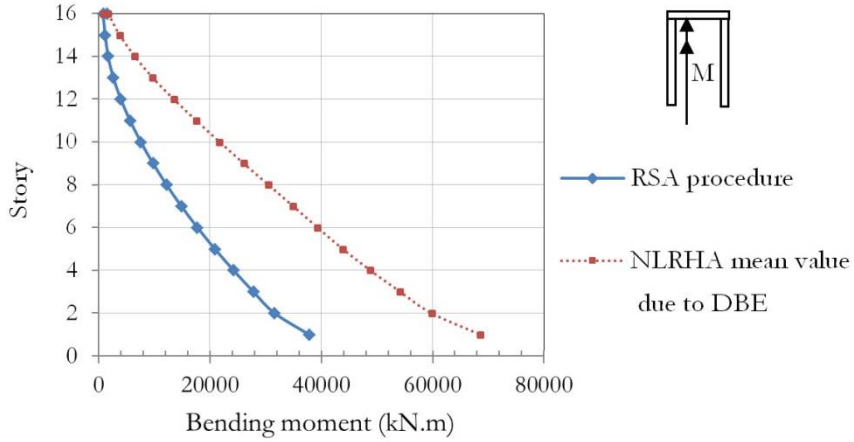

Fig. 23. Bending moment in W2 – about E-W direction – RSA procedure versus NLRHA due to DBE.

5.2.2. Building performance

To check the performance of the building, MCE ground motions are used in NLRHA. The results are investigated in several aspects. Core wall shear response is particularly critical, whereas the flexural response of the wall elements is evaluated using rotation gage elements included in the model in PERFORM-3D [12] and is within immediate occupancy performance level in ASCE41-06 [13] (Table 9). Column hinge rotations are also very critical; few of them exceed the rotation limit for collapse prevention level set by

ASCE41-06 [13] as shown in Table 10. Story drift ratios in both E-W and N-S directions are not exceeding the limit in the code [3] as illustrated in Fig. 24.

Table 9. Most critical wall hinge rotation.

Earthquake loading	Hinge rotation	ASCE41-06 – Limit		
		IO	LS	CP
Average of 7 ground motions	0.0017	0.002	0.004	0.008
Maximum of 7 ground motions	0.002			

Table 10. Most critical column hinge rotation.

Earthquake loading	Hinge rotation	ASCE41-06 – Limit		
		IO	LS	CP
Average of 7ground motions	0.0183	0.004	0.0135	0.0175
Maximum of 7 ground motions	0.0254			

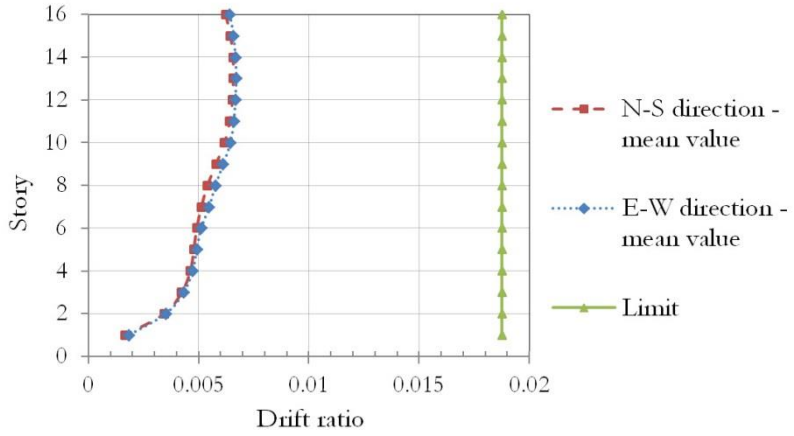

Fig. 24. Maximum story drift ratios in NLRHA due to MCE.

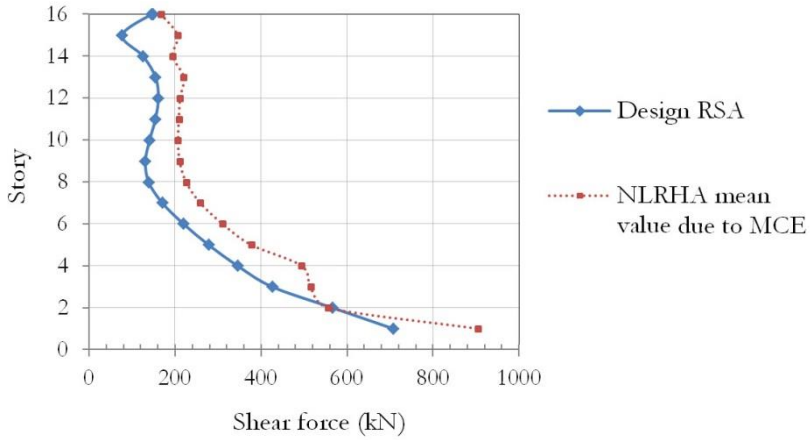

Fig. 25. Shear force in W1 – Design RSA procedure versus NLRHA due to MCE.

DOI:10.4186/ej.2014.18.4.73

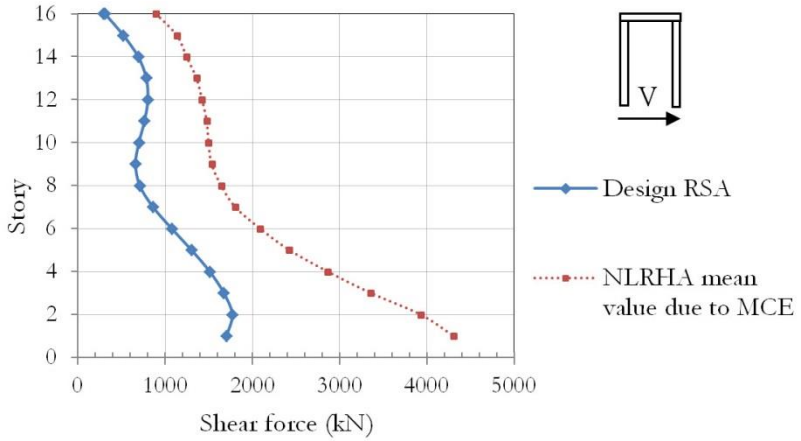

Fig. 26. Shear force in W2 – E-W direction - Design RSA procedure versus NLRHA due to MCE.

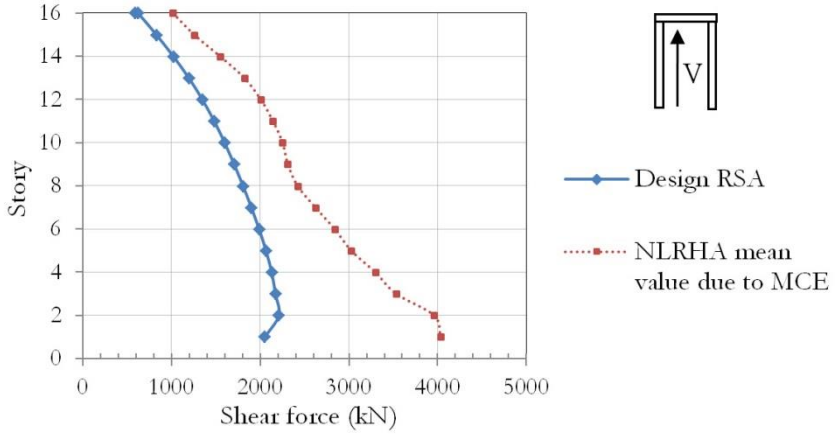

Fig. 27. Shear force in W2 – N-S direction - Design RSA procedure versus NLRHA due to MCE.

Figures 25 through 27 compared the seismic shear demand obtained from mean value of NLRHA of MCE ground motions to the design shear capacity of the shear walls from RSA procedure. It can be interpreted from the figures that the shear demand of the walls exceeds their capacity, which means shear failure could be expected to occur on the walls. It should be noted that the shear design capacity of the walls is obtained from dividing the demands from RSA procedure by a strength reduction factor ϕ of 0.75 [11].

5.3. Modified RSA Procedure

Priestly and Amaris [22] had proposed Modified Modal Superposition (MMS) method to combine the elastic modal shear demand based on two main assumptions: ductility limits primarily first mode response and the inelastic higher modes will not differ significantly from the elastic modes. In MMS method, the elastic seismic shear demand is reduced by a seismic modification factor only in the first vibration mode and then combined with the elastic shear demand of other higher modes into total response. Munir and Warnitchai [9] used a method called uncoupled modal response history analysis (UMRHA) adapted from Chopra and Goel [23] to decompose the inelastic seismic responses into the contribution of each vibration modes. The results are compared with the demands from RSA procedure (with R=1 and R=5.5) and they found that the demands from UMRHA matched RSA (R=5.5) only in the first mode and reasonably close to RSA (R=1) in other higher modes. Hence, it is wise to adapt the modified RSA procedure to MMS method proposed by Priestly and Amaris [22].

In this modified RSA procedure, R_{eff} must be computed first, and then like RSA procedure, the elastic responses of all significant vibration modes are determined using the elastic response spectrum in Fig. 14 (R_{eff} = 1), next only the responses of the first translational mode (E-W direction) and the first torsional

mode of the structure are reduced by the effective seismic modification factor "R_{eff}", finally the responses of all modes are combined into total responses by CQC rule.

As depicted in Fig. 28 through Fig. 30, the shear demands from this modified RSA and RSA procedure are then compared with the corresponding demands evaluated as the average value of the demands in NLRHA employing the set of DBE ground motions. The results show that this modified RSA procedure overestimates the seismic shear demands in W1 and W2 (N-S direction) and that good agreement of shear demands in W2 (E-W direction) from modified RSA and NLRHA is found.

Fig. 31 through Fig. 33 shows that the shear capacity of the walls designed by modified RSA procedure is greater than the mean demand from NLRHA except in the mid-height of W2. So this modified RSA procedure could be used to avoid shear failure in the wall elements. It is noted that the design modified RSA and RSA from Fig. 31 to Fig. 33 are the shear capacities obtained from dividing the shear demands from modified RSA and RSA procedure in Fig. 28 to Fig. 30 by a strength reduction factor ϕ of 0.75 [11].

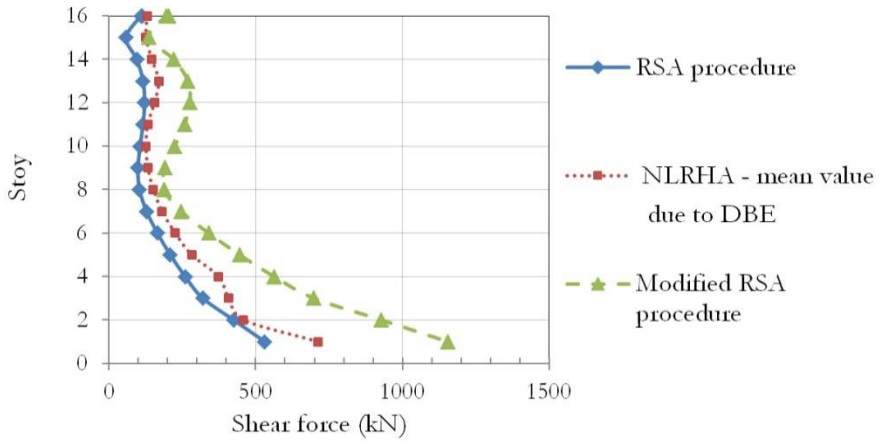

Fig. 28. Shear force in W1 - RSA versus Modified RSA versus NLRHA procedure due to DBE.

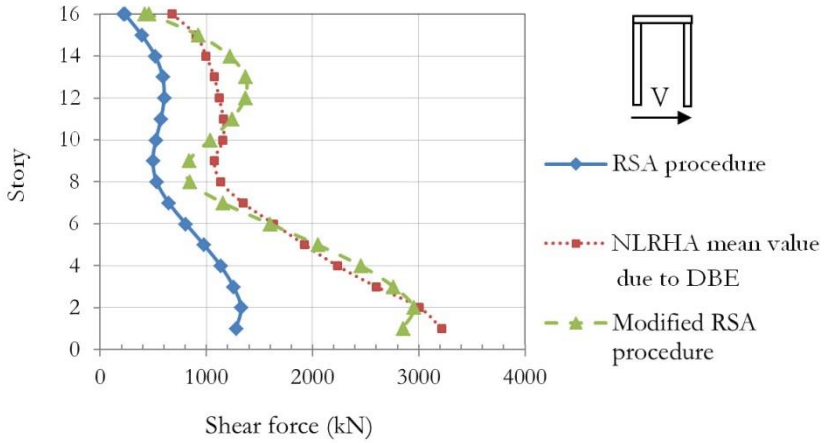

Fig. 29. Shear force in W2 – E-W direction - RSA versus Modified RSA versus NLRHA procedure due to DBE.

DOI:10.4186/ej.2014.18.4.73

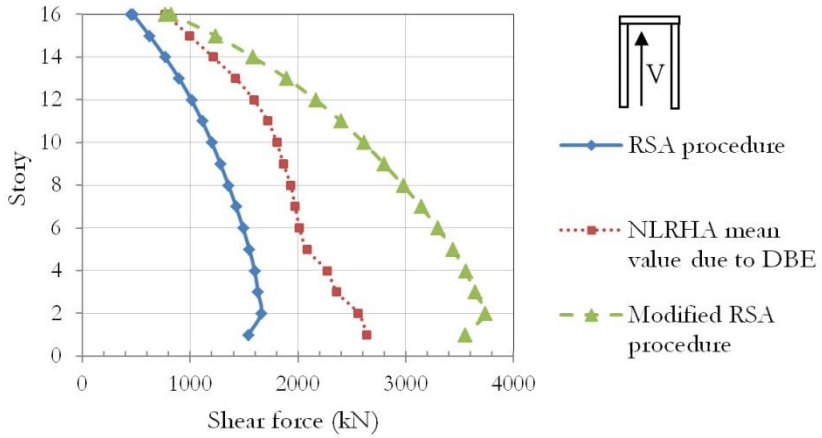

Fig. 30. Shear force in W2 – N-S direction - RSA versus Modified RSA versus NLRHA procedure due to DBE.

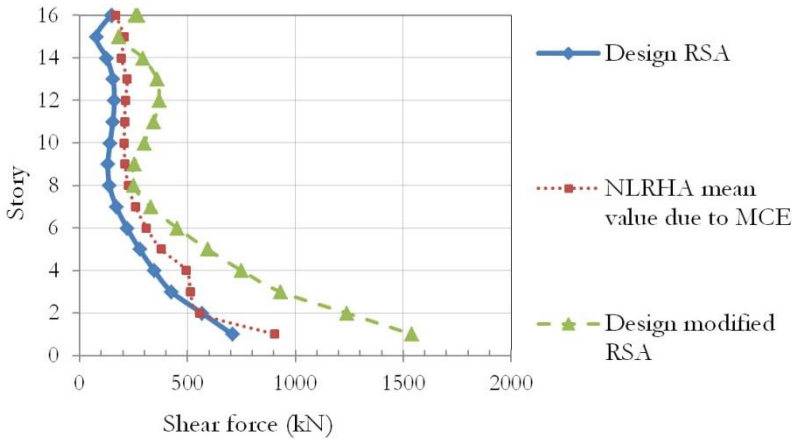

Fig. 31. Shear force in W1 - Design RSA versus Design Modified RSA versus NLRHA procedure due to MCE.

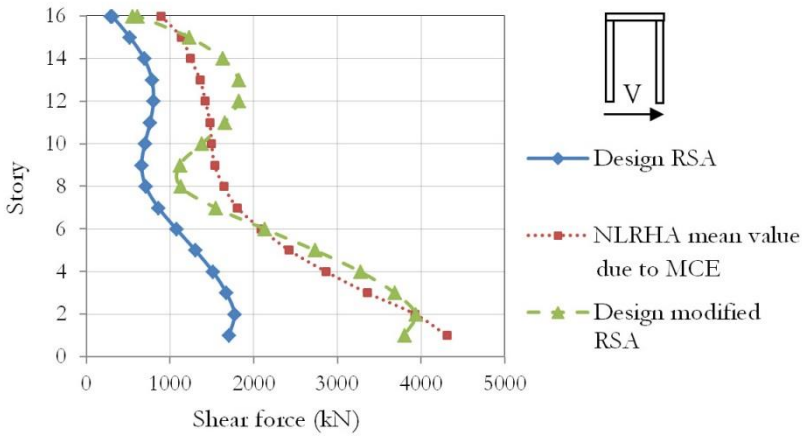

Fig. 32. Shear force in W2 – E-W direction - Design RSA versus Design Modified RSA versus NLRHA procedure due to MCE.

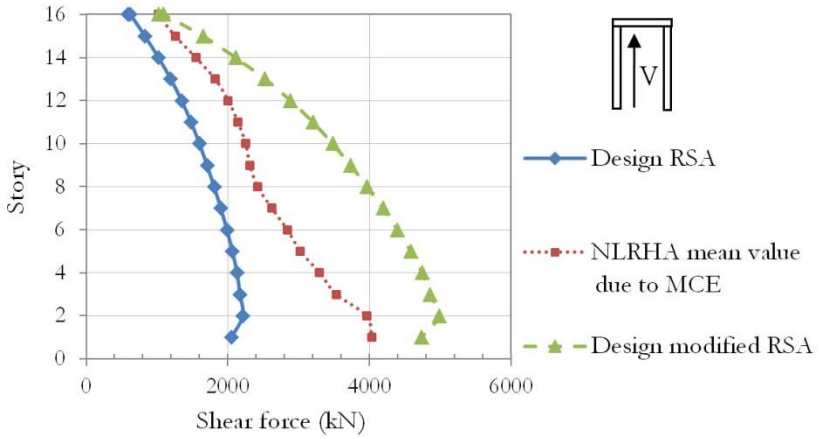

Fig. 33. Shear force in W2 – N-S direction - Design RSA versus Design Modified RSA versus NLRHA procedure due to MCE.

It should be noted that this modified RSA procedure is used to improve the seismic shear demand, hence seismic shear capacity of shear walls only, no modification is necessary in computing deformations and bending moment of the wall elements.

Fig. 34 through Fig. 36 shows the ratio between the shear demands obtained from RSA procedure and the corresponding shear demands from NLRHA procedure for W1 and W2. The average ratio for W1 and W2 in N-S direction is about 1.5, while this ratio is around 2 for W2 in E-W direction.

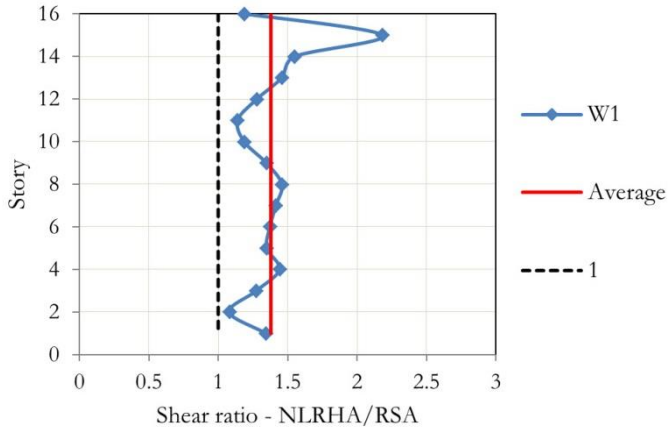

Fig. 34. The ratio of shear demand from NLRHA over RSA procedure – W1.

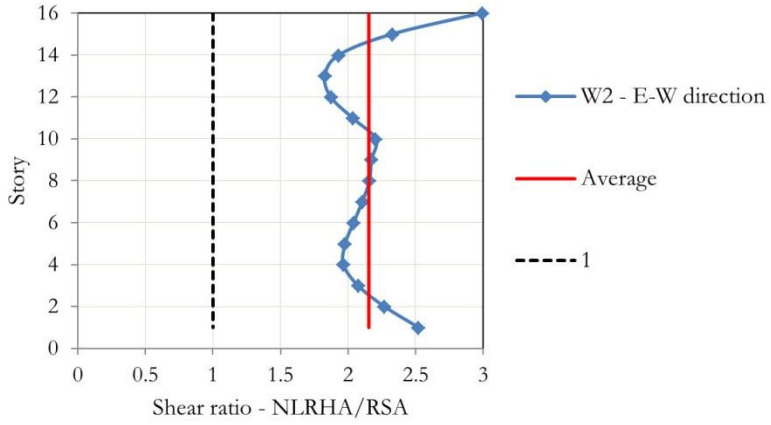

Fig. 35. The ratio of shear demand from NLRHA over RSA procedure – W2 – E-W direction.

DOI:10.4186/ej.2014.18.4.73

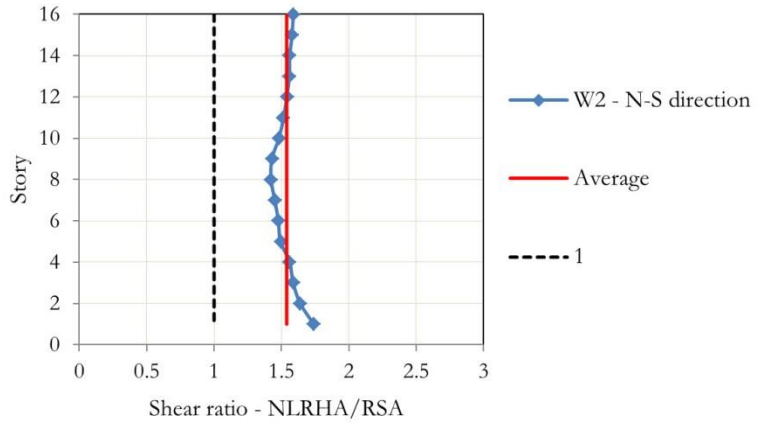

Fig. 36. The ratio of shear demand from NLRHA over RSA procedure – W2 – N-S direction.

Based on these shear demand ratios, we can try to scale the shear demands from RSA procedure to match the high demands from NLRHA procedure using the scaling factor of 1.5 and 2. The results are shown in Fig. 37 through Fig. 39. We can observe that scaling factor of 1.5 can reasonably match the shear demand from RSA to that from NLRHA procedure for the case of W1 and W2 – N-S direction while the this scaling factor is increased to 2 for the case of W2 – E-W direction.

Another observation is that by simply scaled the shear demand from RSA procedure, the shear demand on the walls is even better predicted compared to the modified RSA procedure. Moreover, the shear pattern throughout the entire height of the wall is closer to the shear pattern from NLRHA procedure compared with the modified RSA procedure as illustrated in Fig. 38. So this simple method can serve as an alternative method for predicting shear demand on the walls. It should be noted that scaling the demands from RSA procedure by a factor of 1.5 is equivalent to applying RSA procedure using R = 5.5/1.5 = 3.67, similarly for a factor of 2, R = 5.5/2 = 2.75.

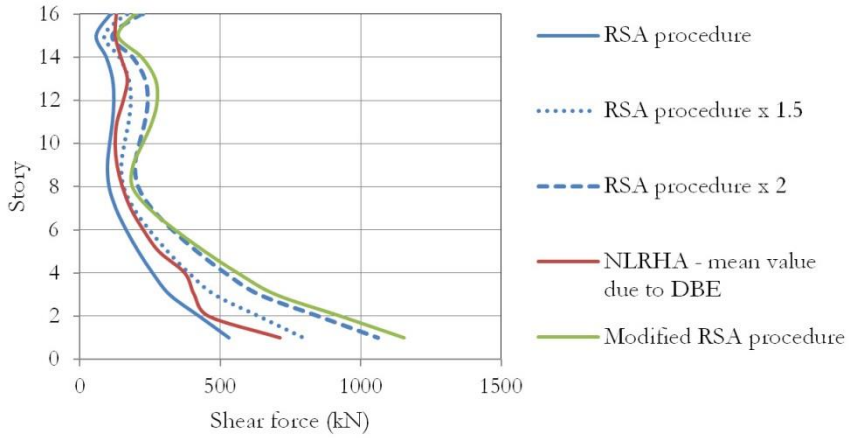

Fig. 37. Shear force in W1 – RSA versus RSA x 1.5 versus RSA x 2 versus Modified RSA versus NLRHA procedure due to DBE.

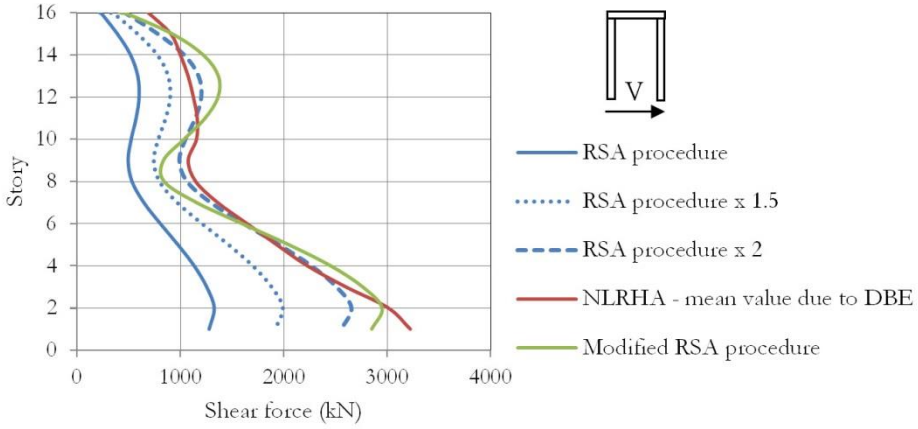

Fig. 38. Shear force in W2 – E-W direction – RSA versus RSA x 1.5 versus RSA x 2 versus Modified RSA versus NLRHA procedure due to DBE.

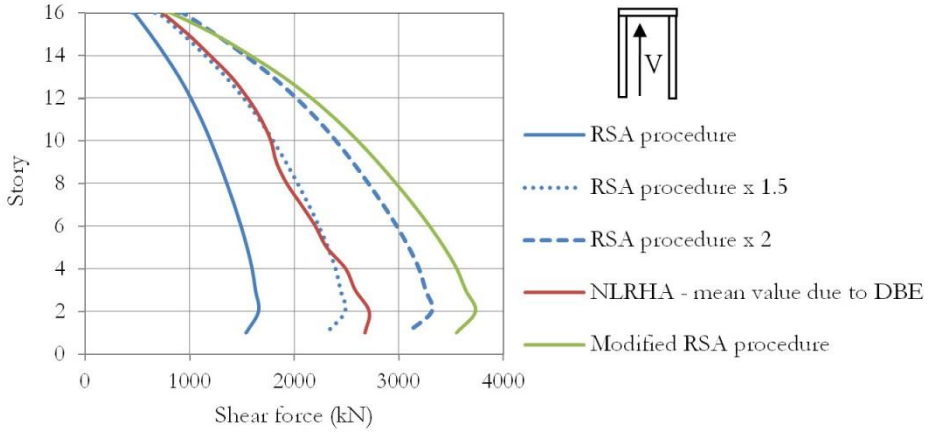

Fig. 39. Shear force in W2 – N-S direction – RSA versus RSA x 1.5 versus RSA x 2 versus Modified RSA versus NLRHA procedure due to DBE.

6. Conclusions

This study has investigated the response spectrum analysis procedure mentioned in the code to design a 16-story case-study building by comparing the demands from RSA with those from NLRHA procedures and allowable limit from the code provision. Based on the results of these comparisons, the following conclusions can be drawn:

1. RSA procedure prescribed in the current Thai seismic design code (based on ASCE7-05 underestimates the demands in shear wall elements. The best estimation of seismic demands obtained from NLRHA could be as high as 2 time the corresponding demands from RSA procedure for wall 2 throughout the entire height of the wall. Moreover, RSA procedure underestimates the drift ratios in E-W direction, which is predominated by frame action, and overestimates the drift ratios in N-S direction, which is predominated by wall action

2. For the performance of the building, inelastic analysis results show that seismic shear failure is expected to occur in the shear wall elements whereas the flexural responses of the wall measured in term of wall rotation satisfy all performance levels namely immediate occupancy (IO), life safety (LS) and collapse prevention (CP) performance levels. The most critical plastic hinge rotation of the columns exceeds admissible rotation from the code for the CP performance level. The maximum story drift ratios of the building in both E-W and N-S directions are within the limit set by ASCE07-05.

3. To avoid shear failure in the shear wall elements, a modified RSA procedure adapted from Priestly and Amaris [22] has been implemented. In this new method, only the responses of the first vibration mode of the translational and torsional mode are divided by "R_{eff}". The results indicate that this new method

works quite well in estimating the force demands in shear walls. However, more researches on different building configurations are needed to confirm the sufficiency of this modified RSA procedure.

4. An alternative RSA method, in which the seismic modification coefficient R is reduced from 5.5 to 3.67 and 2.75, can even predict the shear demands better than those obtained from modified RSA procedure.

Acknowledgements

The authors would like to acknowledge the financial support provided by JICA through the ASEAN University Network/Southeast Asia Engineering Education Development Network (AUN/SEED-Net) program.

References

[1] J. Maffei and N. Yuen. (2007). Seismic performance and design requirements for high rise buildings. *Structural Magazine*. [Online]. pp. 28-32. Available: http://www.structuremag.org/article.aspx?articleID=427.

[2] Department of Public Work and Town & Country Planning, *Thai Seismic Design Code*, DPT 1302-52, 2009.

[3] American Society of Civil Engineers, *Minimum Design Loads for Buildings and Other Structures*, ASCE7-05, 2005.

[4] A. K. Chopra, *Dynamics of Structures: Theory and Applications to Earthquake Engineering*, 3rd ed. Upper Saddle River, NJ: Pearson Prentice Hall, 2007.

[5] A. Zekioglu, M. Willford, L. Jin, and M. Melek, "Case study using the Los Angeles tall buildings structural design council guidelines: 40-storey concrete core wall building," *Structural Design of Tall and Special Buildings*, vol. 16, no. 5, pp. 583-597, 2007.

[6] H. P. Tuan, "Seismic design considerations for tall buildings," M.S. thesis, ROSE School, Pavia, Italy, 2008.

[7] R. Klemencic, J. A. Fry, J. D. Hooper, and B. G. Morgen, "Performance-based design of ductile concrete core wall buildings—issues to consider before detailed analysis," *The Structural Design of Tall and Special Buildings*, vol. 16, no. 5, pp. 599-614, 2007.

[8] C. Sangarayakul and P. Warnitchai, "Approximate modal decomposition of inelastic dynamic responses of wall buildings," *Earthquake Engineering and Structural Dynamics*, vol. 33, no. 9, pp. 999-1022, 2004.

[9] A. Munir and P. Warnitchai, "The cause of unproportionately large higher mode contributions in the inelastic seismic responses of high-rise core-wall buildings," *Earthquake Engineering and Structural Dynamics*, vol. 41, no. 15, pp. 2195-2214, 2012.

[10] Computers and Structures, *ETABS, Extended 3D Analysis of Building Systems Software*, Nonlinear Version 9.7.4, Inc.: Berkeley, CA.

[11] ACI Committee 318, *Building Code Requirements for Structural Concrete and Commentary*, ACI 318-08, 2008.

[12] Computers and Structures, *Perform-3D, Nonlinear Analysis and Performance Assessment for 3D Structures Software*, Version 5.0.0., Inc.: Berkeley, CA.

[13] American Society of Civil Engineers, *Seismic Rehabilitation of the Existing Buildings*, ASCE41-06, Alexander Bell Drive, Reston, Virginia, 2006.

[14] C. B. Haselton, A. B. Liel, S. T. Lange, and G. G. Deierlein, "Beam-column element model calibrated for predicting flexural response leading to global collapse of RC frame buildings," Pacific Earthquake Engineering Research Center, College of Engineering, UC Berkeley, PEER Report 2007/03, May 2008.

[15] T. B. Panagiotakos and M. N. Fardis, "Deformations of reinforced concrete members at yielding and ultimate," *ACI Structural Journal*, vol. 98, no. 2, pp. 135-148, 2001.

[16] M. K. M. Reddiar, "Stress-strain model of confined and unconfined concrete and stress-block parameters," M.S. thesis, Texas A&M University, USA, 2009.

[17] J. B. Mander, M. J. N. Priestley, and R. Park, "Theoretical stress-strain model for confined concrete," *Journal of Structural Engineering*, vol. 114, no. 8, pp. 1804-1826, August 1988.

[18] T. Kaewnurachadasorn, "Seismic evaluation and retrofit of a bridge," M.S. thesis, Department of Civil Engineering, Faculty of Engineering, Chulalongkorn University, 2012 (in Thai).
[19] H. Sezen, "Seismic behavior and modeling of reinforced concrete building columns," Ph.D. thesis, UC Berkeley, USA, 2000.
[20] EduPro Civil System, *ProShake Ground Response Analysis Program, User's Manual,* Version 1.1, Inc, Redmond, Washington.
[21] Faculty of Engineering, Chulalongkorn University, *Seismic Evaluation of Reactor Pool No.1 and Its Housing Structure Submitted to Thailand Institute of Nuclear Technology* (Public organization), 2010.
[22] N. Priestly and A. Amaris, "Dynamic amplification of seismic moments and shear forces in cantilever walls," in *Proceedings of FIB Symposium, Concrete Structures in Seismic Regions*, Athens, 2003.
[23] A. K. Chopra and R. K. Goel, "A modal pushover analysis procedure for estimating seismic demands for buildings," *Earthquake Engineering and Structural Dynamics*, vol. 31, no. 3, pp. 561-582, 2002.